Int. J. Environ. Res., 8(3):741-750,Summer 2014
ISSN: 1735-6865

Removal of Heavy Metal by Nickel Oxide Nano Powder

Abd El fatah, M.[1*] and Ossman, M.E.[1,2]

[1]Petrochemical Engineering Department, Faculty of Engineering, Pharos University, Alexandria, Egypt

[2] City for Scientific Research and Technology Application (SRTA-City), Alexandria, Egypt

Received 17 Oct. 2013; Revised 3 Jan. 2014; Accepted 7 Jan. 2014

ABSTRACT: In this study metal oxide nano powder namely NiO nanopowder was prepared .The produced metal oxide was characterized and used as potential adsorbent for the removal of Pb and Zn from aqueous solution. The rate of uptake of the Pb and Zn are rapid in the beginning and the time required for equilibrium adsorption is 120 min .The time of equilibrium as well as time required to achieve a definite fraction of equilibrium adsorption is independent of initial concentration. The results showed that the removal of Pb increased significantly as the pH increased from 2.0 to 6.0 and approach a plateau at pH range of 6.0–9.0., while the removal of Zn increased significantly as the pH increased from 2.0 to 9.0. The adsorption of pb onto NiO follows the Langmiur isotherm, while the adsorption of Zn onto NiO follows the Freundlish isotherm . The pseudo second order kinetic model provided good correlation for the adsorption of Pb onto NiO nanopowder while the pseudo first order kinetic model provided good correlation for the adsorption of Zn onto NiO nanopowder.

Key words: Heavy metals, Nanopowder, Adsorption, Metal oxide, Kinetic, Isotherm

INTRODUCTION

Nanotechnology is an emerging science with wide applications in the remediation of environmental pollutants. In recent years, a great deal of attention has been focused on the synthesis and application of nanostructure materials as adsorbents or catalysts to remove toxic and harmful substances from water and air. Reactive nanoparticles have a significant amount of surfaces and thus attract much interest to be applied as adsorbents in comparison to macromolecules (Uzaira *et al.,* 2012). Heavy metals are the most important constituents among toxic compounds in the effluents (Wang *et al.,* 2000). Although at low doses some heavy metals are essential micronutrients for plants and animals, being responsible for biochemical, immunological and physiological activities (Yemane *et al.,* 2008, He *et al.,* 2005), in higher doses they can detrimentally affect the health of most living organisms (Gheorghiu, *et al.,* 2007).

Lead can be found in water as a result of human activities, such as fossil fuel burning, mining, and manufacturing, lead and lead compounds can be found in all parts of our environment (Kannan, *et al.,* 2009), Also zinc is used in metal alloys such as stainless steel; protective coatings on metal (electroplating); magnetic tapes; and pigments for paints, batteries and other materials (El-Sayed, *et al.,* 2011). Different treatment techniques for wastewater laden with heavy metals have been developed in recent years both to decrease the amount of wastewater produced and to improve the quality of the treated effluent. The main techniques, which have been utilized to reduce the heavy metals content of effluents, include ion-exchange (Pehlivan *et al.,* 2007), membrane processes (Maximous *et al.,* 2010), Precipitation(Steven *et al.,* (2005), Membrane filtration(Moussa *et al.,* 2004) ,electrolytic methods (Widner *et al.,* 1997)and adsorption using different adsorbents such as Activated carbon (Ossman et. al. 2013,Asrari *et al.,* 2010, Shipley *et al.,* 2013), (Kannan N *et al.,* 2009, Mehrasbi *et al.,* 2008, Devaprasath *et al.,* 2007), Agricultural waste (Shanmugavalli R *et al.,* 2009) , peanut skins (Reddad *et al.,* 2002), pecan shell-based granular activated carbons (Bansode *et al.,* 2003), modified rice husk (Wong *et al.,* 2003). maize stalks (El-Sayed *et al.,* 2011). Metal oxides play a significant role in many fields of nanotechnology including nanocatalysis, sensing, supermagnetic properties,

*Corresponding author E-mail: marwa.abdelfattah@pua.edu.eg

nanoenergy storage and conversion, fuel cells, and electroceramics (Bao *et al.,* 2001; Gao *et al.,* 2001; Braos-García *et al.,* 2003; Liang *et al.,* 2004; Seto *et al.,* 2005; Tian *et al.,* 2005; Jeon *et al.,* 2005,2006) . Also, metal oxide can be used in adsorption such as boehmite (Abu-Elella.*et al.,* 2013).

The aim of this work is to produce a new adsorbent (Metal oxide nano powder namely NiO nano powder,) then use it as adsorbent for removal of Pb and Zn and study the effect of different variables such as contact time, adsorbent dosage, pH, metal ion concentration on the adsorption process.

MATERIALS & METHODS

All chemicals used in the experiments are analytic reagent grade. Nickel sulphate $\{NiSO_4(H_2O)_6\}$ and oxalic Acid$\{H_2C_2O_4\}$ for preparing nickel oxalate $\{NiC_2O_4.2H_2O\}$, Polyethylene glycol, Distilled water and Acetone. The preparation of nickel oxalate by dissolving equimolar quantity of nickel sulphate and oxalic Acid in minimum amount of water. This mixture was well stirred in a conical flask by using a magnetic stirrer at 400 rpm. The light green precipitate of nickel oxalate dehydrates \was filtered through sintered glass funnel and washed with distilled water. Finally, it was washed with dry acetone and dried under vacuum. The prepared nickel oxalate was mixed with Polyethylene glycol in the weight 1:5. The resultant mixture was placed in crucible and ignited at 350°C to give NiO as a residue. On cooling to room temperature, no traces of carbon impurities were observed in the final residue of NiO. The surface morphology of the NiO nano powder was analyzed using different magnifications by scanning electron microscopy (SEM, JEOL JSM 6360LA). The surface functional groups with binding sites and structure of the solid materials were studied by Fourier Transform Infrared Spectroscopy (FTIR-8400S, Shimadzu). The FT-IR spectrum of NiO nano powder was recorded in its normal range . The XRD(X-ray diffraction) of the NiO nano powder was analyzed using Shimadzu XRD-7000 .

A stock solution of Lead nitrate (1000 ppm) was prepared by dissolving 1.6 gm of 99% $Pb(NO_3)_2$ in 1L of distilled water. While 1000 mg/L of zinc stock solution was prepared by dissolving 4.397 g of $ZnSO_4{\cdot}7H_2O$ in 1 L distilled water. Equilibrium isotherms for lead and zinc were obtained by performing batch adsorption studies. Solutions of 250 ppm were adjusted to optimum pH values and adsorbent doses ranging between 0.1 and 1 g were added to solutions. The adsorbed heavy metal amount (q_e) per unit absorbent mass was calculated as follows:

$$q_e = \frac{(C_0 - C_e) * V}{W} \quad (1)$$

Where C_o is the initial heavy metal concentration (ppm), C_e is the concentration of heavy metal at equilibrium (ppm), W is the adsorbent dosage (mg) and V is the solution volume (L).

RESULTS & DISCUSSION

SEM images with magnification factor 3500 for Nickel oxide nano powder are taken in order to show the major features of the nanopowder morphology. Fig. 1 showed the SEM for Nickel oxide nano powder. Fig ,1 (a) and (b) indicated that mono-dispersive and highly crystalline NiO nanoparticles are obtained. The appearances of the particles are in spherical shape, the particles are highly agglomerated and they are essentially cluster of nanoparticles. The diameter of the particle observed from SEM analysis is ranged from 38 -130 nm. The fine particle size resulted in a large surface area (191 m^2/g) that in turn, enhances the nanoparticles catalytic activity. The surface area of NiO nano powder was determined by nitrogen gas adsorption after 24 h degassing at 77.4 K. The BET equation was used to calculate the surface area.

Fig,2 showed Fourier transformed spectrum of NiO nano particles at room temp. The spectrum was recorded in its range .The FTIR spectrum showed the characteristics peaks at 575.41/cm, 677.04 /cm ,1635.45.90 /cm, 2921.97 /cm, 3440.29 / cm. The band at 575.41/ cm revealed the presence of NiO. The peaks at 1629.90 /cm, 3431.48 /cm represented that the sample contained traces of water. The serrated absorption bands in the region of 1000– 1500/ cm are assigned to the O–C=O symmetric and asymmetric stretching vibrations and the C–O stretching vibration, but the intensity of the band has weakened, which indicated that the sample contains no impurity of carbon. Fig.(3) showed the X-ray diffraction (XRD) for NiO nanoparticles. It can be seen from Fig.(3) that the peaks appearing at 2θ = 37.3º, 43. 3º, and 63.18º which are indexed as (111), (200), and (220) respectively and represents face-centered cubic (FCC) crystalline structure of nickel oxide. All these diffraction peaks showed typical NiO pattern when compared with the Shimadzu XRD-7000 card in the conventional way. The XRD pattern shows that the sample is single phase and no any other impurities diffraction peak except the characteristic peaks of FCC phase nickel oxide was detected.

In order to establish equilibrium time for maximum uptake and to know the kinetics of adsorption process, the adsorption of Pb and Zn on NiO nanopowder as adsorbents was studied as a function of contact time and results are shown in Fig. 4 and Fig.5 respectively. It was found that the rate of uptake of Pb and Zn are rapid in the beginning and 70% adsorption is completed

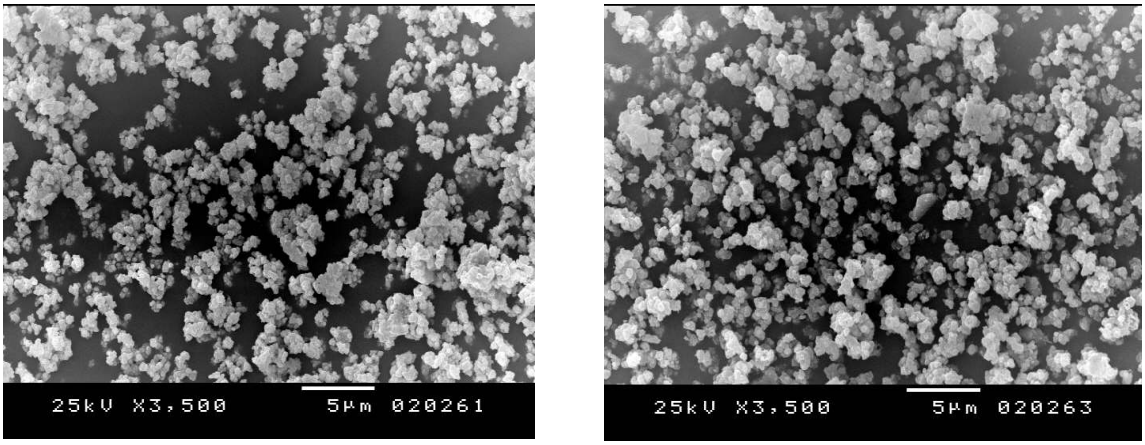

(a) (b)

Fig.1. SEM for Nickel oxide nano powder calcinated at 350 ^{0}C using muffle furnace (b) prepared by adding poly ethylene glycol

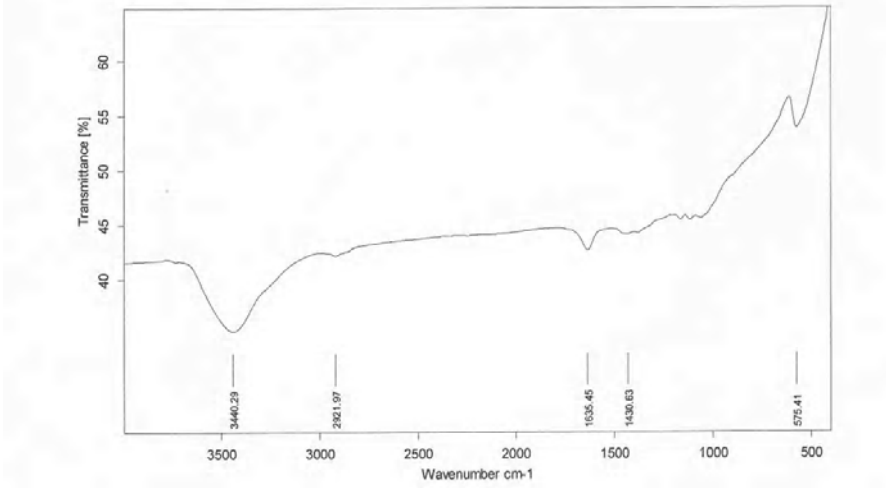

Fig. 2. FTIR for NiO nano powder

within 150 min. and the time required to achieve equilibrium is 120 min.,The results showed that NiO has higher Adsorption capacity for Pb than that for Zn.

The effect of concentration on the equilibration time was also investigated as a function of initial Pb and Zn concentrations. It was found that the time required to reach equilibrium is independent of initial concentration. The acidity of solution (pH) is one of the most important parameters controlling uptake of heavy metals from aqueous solutions. Fig. 6 showed that the removal of Pb increased significantly as the pH increased from 2.0 to 6.0 and approached a plateau at pH range of 6.0–9.0. The removal percentage reached 65% of Pb on NiO nanopowder at pH of 6.0. While Fig.7 showed that the removal percentage of Zn increased significantly as the pH increased from 2.0 to 9.0 and at pH > 9, the solubility of Zn is known to be lowered at higher pH values [Thye *et al.,* 2001]. The results were reflection of adsorption and precipitation processes on NiO nanopowder rather than adsorption only.

The species of Pb in solution at different pH values is the most important for the removal of Pb from aqueous solution to NiO nano powder. At pH < 6, the predominant lead specie is Pb(II) and the removal of Pb(II) is mainly accomplished by sorption reaction. When pH value is low (<3), a high concentration of positively charged protons compete with Pb(II) for exchangeable cations on the surface of NiO nanopowder. As pH value is higher, there would be a dissociation of weak acid, which could make the adsorbent surface negatively charged to attract the positively charged metal ions, and hence the

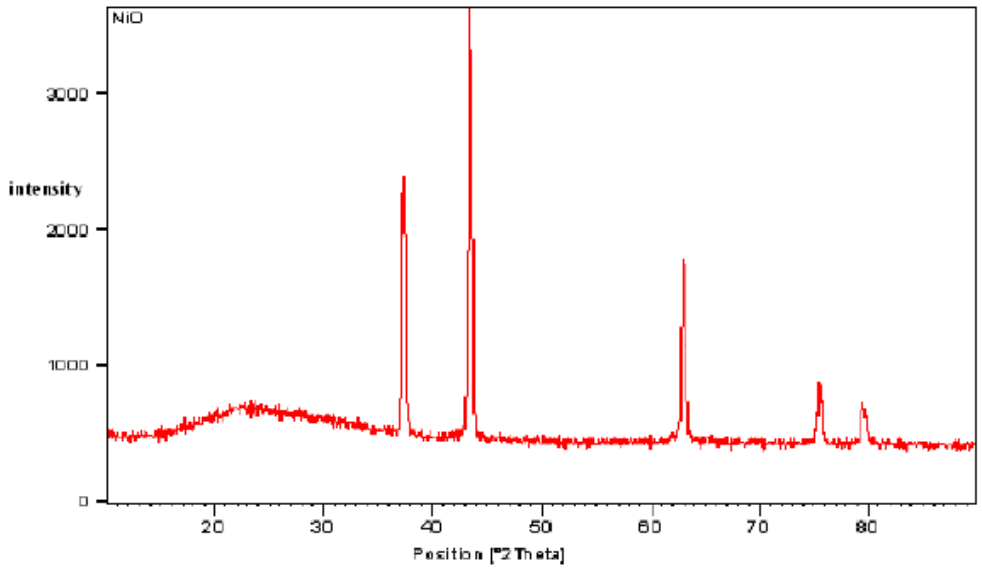

Fig. 3. XRD pattern of NiO nanoparticles

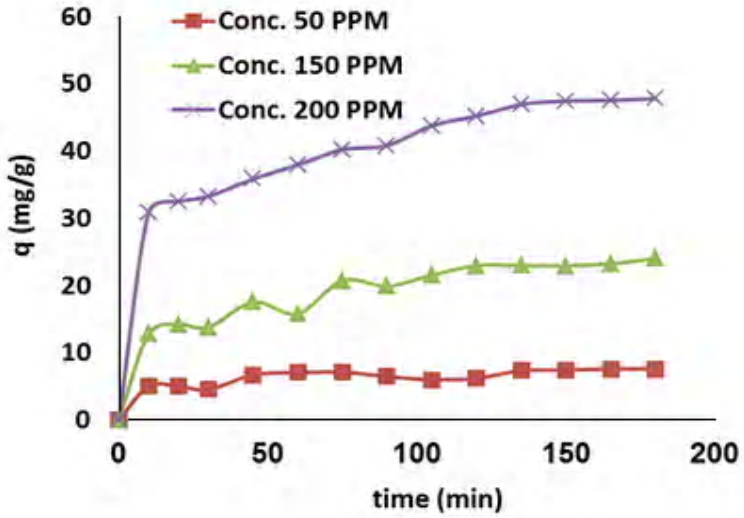

Fig. 5. Effect of contact time on the adsorption capacity of NiO nano powder for Zn at different concentration and pH is 5, adsorbent dosage 2g/l and at 25 ^{0}C

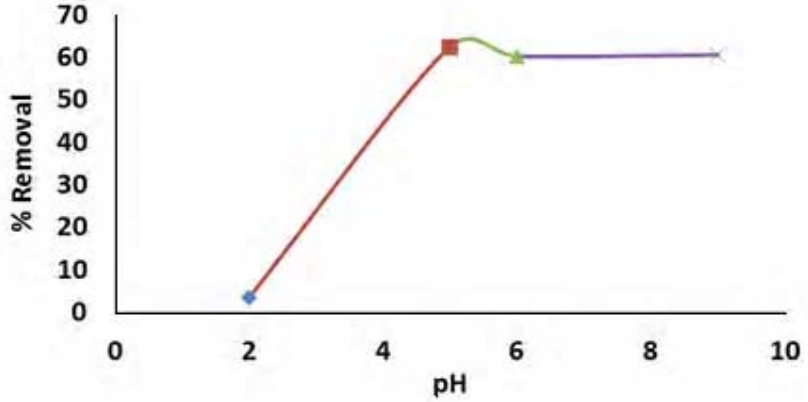

Fig. 6. The effect of pH on the removal of Pb at initial concentration of 100 ppm, adsorbent dosage 2g/l ,and at 25 ^{0}C for 1hr

opportunity of heavy metal binding on adsorbents also increased, resulting in a rapid increase in the adsorption of heavy metal ions (Zeng *et al.,* 2011). It was also noticed that the pH of the metal ion solution decreased after equilibration time for the given metal ion concentration and amount of adsorbent. This change in pH is attributed to the exchange of H^+ ions between the surfaces of NiO nanoparticles and the metal ion solutions. This clearly indicated that process of heavy metal ion adsorption onto the NiO nanoparticles is predominately an ion exchange phenomenon that involves exchange of M^{2+} ions of the solution with H^+ ions of the adsorbent (Mahmood *et al.,* 2011).

The results of the experiments with varying adsorbent dosage are presented in Fig. 8 and Fig.9. Fig. 8 showed that with an increase in the adsorbent dosage from 0.8 to 4.5 g/L, the removal of Pb increased from 60% to 100% while Fig. 9 revealed that the removal of Zn increased from 40% to 45% .This can be explained by the fact that the more mass available the more the contact surface offered to the adsorption. These results are qualitatively in a good agreement with those found in the literature (El-Sayed *et al.,* 2011).

Adsorption isotherms used to determine the capacity and optimizing the use of the adsorbent at equilibrium. Therefore, the correlation of equilibrium data by either theoretical or empirical equations is essential to the practical design and operation of adsorption systems. The analysis of the isotherm data is important to develop an equation which accurately represents the results and could be used for design purposes. In order to investigate the adsorption isotherm, the adsorption data can be interpreted using several relationships which describe the distribution of heavy metal molecules between the aqueous and solid phases. In order to investigate the adsorption isotherm, the experimental data of equilibrium isotherms were interpreted using three equilibrium models; the Freundlich , the Langmuir and Dubinin–Radushkevich (D–R) isotherm. This modeling permits us to determine the maximal capacity of removal.

Langmuir's isotherm model suggests that the uptake occurs on homogeneous surface by monolayer sorption without interaction between adsorbed ions .The linear form of Langmuir isotherm equation is represented by the following equation

$$\frac{C_e}{q_e} = \frac{1}{Q^0 b} + \frac{1}{Q^0} C_e \qquad (2)$$

Where Q^0 is the maximum metal ions uptake per unit mass of adsorbent (mg/g) related to adsorption capacity and b is Langmuir constant (L/mol) related to energy of sorption. Therefore, a plot of C_e/q_e versus C_e, gives a straight line of slope $1/Q^0$ and intercept $1/(Q^0 b)$ as shown in Fig.10,11 for adsorption of Pb and Zn onto NiO nano powder respectively.

Freundlich isotherm describes the adsorption equation that involves heterogeneous adsorption .This empirical isotherm is expressed by the following equation:

$$q_e = K_F C_e^{1/n} \qquad (3)$$

The equation is conveniently used in the linear form by taking the logarithm of both sides as

$$\log q_e = \log K_F + \frac{1}{n} \log C_e \qquad (4)$$

Freundlich constants, K_F and 1/n, are related to adsorption capacity and intensity of adsorption, respectively. The values of n and K_F can be calculated from the slope and intercept of the plot of log q_e versus log C_e derived from Eq. (4). The magnitude of the exponent 1/n gives an indication of the favorability of adsorption. The applicability of the Freundlich sorption isotherm was also analyzed, using the same set of experimental data, by plotting log (qe) versus log(Ce) as shown in Fig.12, 13 for adsorption of Pb and Zn onto NiO nano powder respectively.

A comparison of correlation coefficients for the isotherms is listed in Table 1. The correlation coefficient, R^2, for the Langmuir isotherm is greater than that for the Freundlich isotherm in case of adsorption of Pb, while it is clear that the Freundlich isotherm has best fitted for the adsorption data of Zn onto NiO. Freundlich plots have high linearity (>0.940) which indicate that the process conformed to the empirical Freundlich pattern of adsorption on non-specific, energetically non-uniform, heterogeneous surface in terms of functional groups. Dubinin–Radushkevich isotherm is generally applied to express the adsorption mechanism with a Gaussian energy distribution onto a heterogeneous surface (Dabrowski 2001, Gunay *et al.,* 2007) as shown in Fig.12. The model has often successfully fitted high solute activities and the intermediate range of concentrations datawell. The D–R isotherm does not assume a homogeneous surface or constant sorption potential. The D–R model been applied in the following Eq. (5) and its linear form can be shown in Eq. (6):

$$q_e = q_m \exp(-K_{ad} \epsilon^2 \qquad (5)$$

$$\ln(q_e) = \ln(q_m) - K_{ad} \epsilon^2 \qquad (6)$$

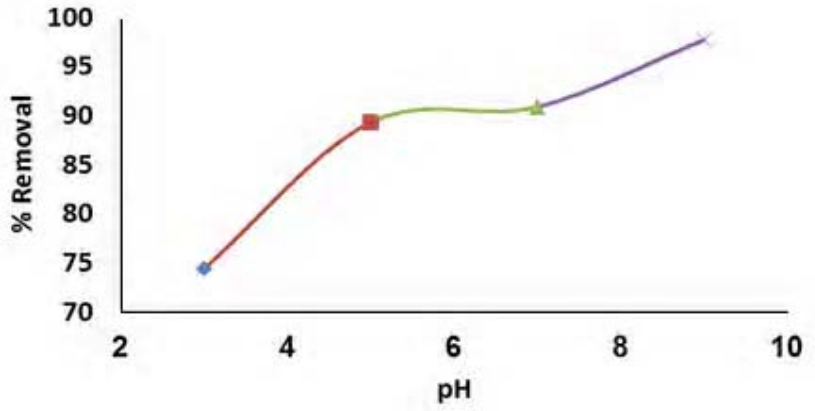

Fig. 7. The effect of pH on the removal of Zn at initial concentration of 100 ppm, adsorbent dosage 2g/l ,and at 25 ^{0}C for 1hr

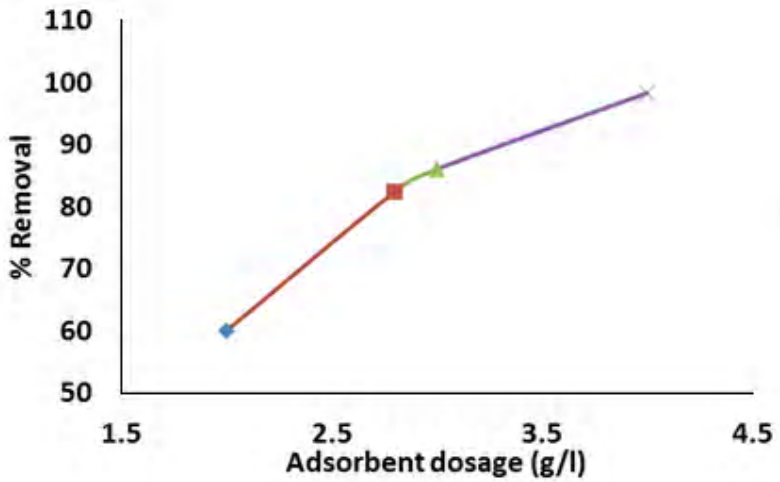

Fig. 8. Effect of dosage of adsorbent on the removal efficiency,%, of Pb ions using NiO nano powder (Initial concentration of Pb 100 ppm, pH= 5 and Contact time: 1 h)

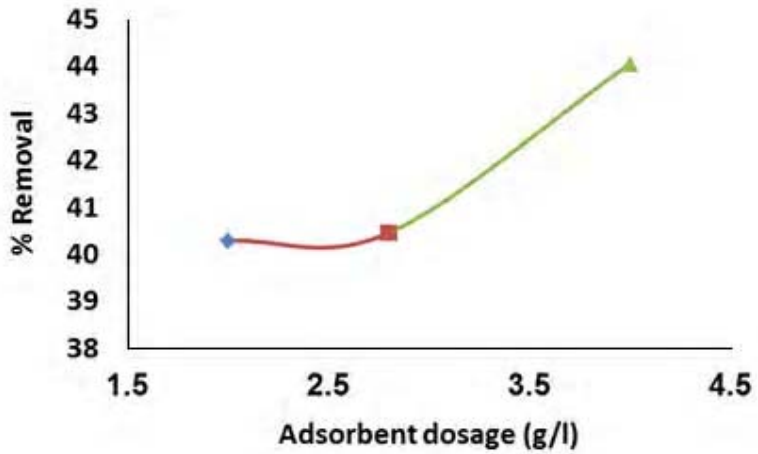

Fig. 9. Effect of dosage of adsorbent on the removal efficiency,%, of Zn ions using NiO nano powder (Initial concentration of Zn 100 ppm, pH= 5 and Contact time: 1 h)

Table 1. Langmuir and Freundlish models for the removal of Pb and Zn onto NiO nano powder

Isotherm model		
Langmuir	Removal of Pb	Removal of Zn
Qm (mg g^{-1})	50.505	63.694
Ka (L mg^{-1})	0.101	0.017
No. of parameter estimated	2	2
Data point available	4	4
R^2	0.9761	0.872
Freundlich		
1/n	*0.187*	*0.5524*
KF (mg g^{-1})	18.791	3.295
No. of parameter estimated	2	2
Data point available	4	4
R^2	0.9638	0.9461
Dubinin–Radushkevich q_m (mg g^{-1})	48.66	50.5
$\in (KJ/mol)$	0.07	0.098
No. of parameter	2	2
Data point available	4	4
R^2	0.9824	0.0965

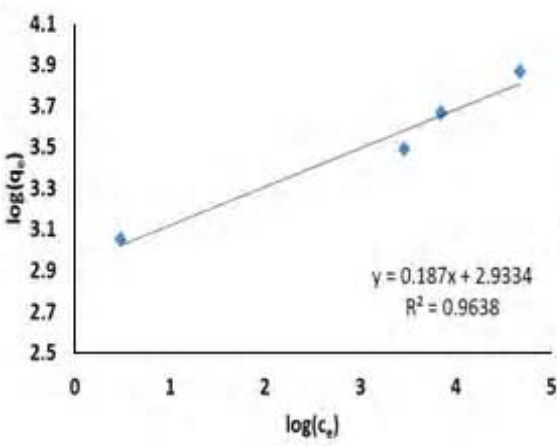

Fig. 10. Langmiur isotherm for adsorption of Pb onto NiO nano powder

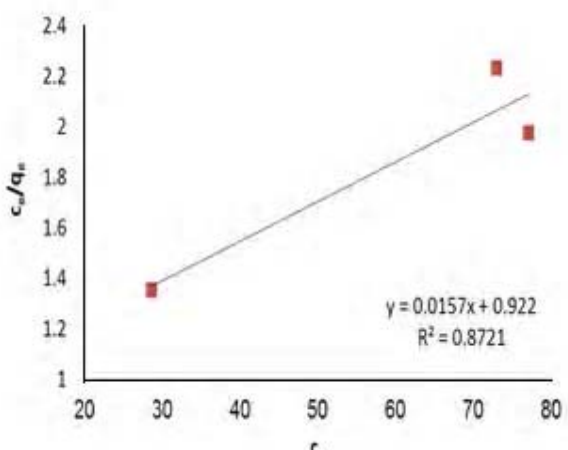

Fig. 11. Langmiur isotherm for adsorption of Zn onto NiO nano powder

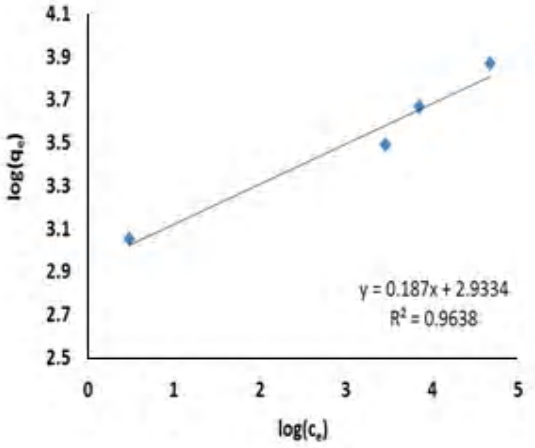

Fig. 12. Freundlish isotherm for adsorption of Pb onto NiO nano powder

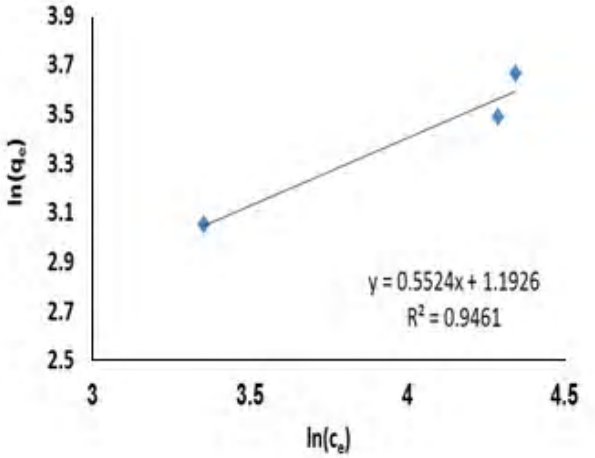

Fig. 13. Freundlish isotherm for adsorption of Zn onto NiO nano powder

where K_{ad} is a constant related to the adsorption energy, q_m is the theoretical saturation capacity, and $\in$ the Polanyi potential calculated from Eq. (7).

$$\in = RT\ln\left[1+\frac{1}{C_e}\right] \quad (7)$$

The slope of the plot of ln qe vs. $\in^2$ gives K (mol²/(kJ²) and the intercept yields the adsorption capacity, q_m (mg /g). The calculated value of D–R parameters is given in Table 1. The saturation adsorption capacity q_m obtained using D–R isotherm model for adsorption of Pb and Zn onto NiO nanopowder are 48.66 mg /g and 50.5 mg/ g respectively and the the mean free energy, $\in$= 0.07KJ/mol and 0.0980 KJ/mol respectively which indicating a physio-sorption process. Kinetics of adsorption is one of the most important characteristics to be responsible for the efficiency of adsorption. The adsorbate can be transferred from the solution phase to the surface of the adsorbent in several steps and one or any combination of which can be the rate-controlling mechanism: (i) mass transfer across the external boundary layer film of liquid surrounding the outside of the particle; (ii) diffusion of the adsorbate molecules to an adsorption site either by a pore diffusion process through the liquid filled pores or by a solid surface diffusion mechanism; and (iii) adsorption (physical or chemical) at a site on the surface (internal or external) and this step is often assumed to be extremely rapid.

The overall adsorption can occur through one or more steps. In order to investigate the mechanism of process and potential rate controlling steps, the kinetics of Fe(III) adsorption onto activated carbon were analyzed using pseudo-first-order (Lagergren et al., 1898), pseudo-second-order (Ho 2000), Elovich (Chien *et al.,* 1980), and fractional power (Weber *et al.,* 1963, Srinivasan *et al.,* 1988) kinetic models. The conformity between experimental data and the model predicted values was expressed by the correlation coefficients (R^2, values close or equal to 1).

The adsorption kinetic data were described by the Lagergren pseudo-first-order model (Lagergren *et al.,* 1898), which is the earliest known equation describing the adsorption rate based on the adsorption capacity. The linear form equation is generally expresses a follows:

$$\log(q_e - q_t) = \log q_e - \frac{K_1}{2.303}t \quad (8)$$

In order to obtain the rate constants, the values of log (q_e _q_t) were linearly correlated with *t* by plot of log (*q*e _*qt*) versus *t* to give a linear relationship from which K_1 and predicted q_e can be determined from the slope and intercept of the plot, respectively. The variation in rate should be proportional to the first power of concentration for strict surface adsorption. However, the relationship between initial solute concentration and rate of adsorption will not be linear when pore diffusion limits the adsorption process. The adsorption kinetic may be described by the pseudo-second order model. The linear equation is generally given as follows:

$$\frac{t}{q_t} = \frac{1}{K_2}\frac{1}{q_e^2} + \frac{1}{q_e}t \quad (9)$$

If the second-order kinetics is applicable, then the plot of t/q_t versus *t* should show a linear relationship. Values of K_2 and equilibrium adsorption capacity q_e were calculated from the intercept and slope of the plots of t/q_t versus *t*. The linear plots of t/q_t versus *t*

show good agreement between experimental and calculated q_e values (Table 2). The correlation coefficients for the pseudo second-order kinetic model are greater than 0.93, which led to believe that the pseudo second order kinetic model provided good correlation for the adsorption of Pb onto NiO nanopowder while the pseudo first order kinetic model provided good correlation for the adsorption of Zn onto NiO nanopowder.

Table 2. Kinetic parameters for the adsorption of Zn and Pb onto NiO nano powders

Kinetics models	Pb on NiO	Zn on NiO
Pseudo first order kinetics		
K_1(min)	0.0164	0.0241
q_1(mg/g)	13.401	21.538
R_1^2	0.8014	0.7724
Pseudo second order kinetics		
K_2(g/mg min)	0.0026	0.0029
q_2(mg/g)	33.898	8.19
R_2^2	0.9933	0.626

CONCLUSION

Metal oxide nano powders namely NiO nanopowder was prepared .The produced metal oxide was characterized and used as potential adsorbent for the removal of Pb and Zn from aqueous solution.The rate of uptake of the Pb and Zn are rapid in the beginning and the time required for equilibrium adsorption is 120 min., and it is found that NiO has higher Adsorption capacity for Pb than for Zn. The time of equilibrium found to be independent of initial concentration. The results showed that the removal of Pb increased significantly as the pH increased from 2.0 to 6.0 and approach a plateau at pH range of 6.0–9.0. While the removal of Zn increased significantly as the pH increased from 2.0 to 9.0 and at pH > 9 The results were reflection of adsorption and precipitation processes on NiO nanopowder rather than adsorption only. The adsorption of pb onto NiO followed the Langmiur isotherm while the adsorption of Zn onto NiO followed the Freundlish isotherm .The pseudo second order kinetic model provided good correlation for the adsorption of Pb onto NiO nanopowder, while the pseudo first order kinetic model provided good correlation for the adsorption of Zn onto NiO nanopowder. The study revealed that NiO nanopowder can be a promising adsorbent for the removal of Pb and Zn from waste water.

REFERENCES

Gheorghiu, C., Cable, J., Marcogliese, D. J. and Scott, M. E. (2007). Effects of waterborne zinc on reproduction. Survival and morphometrics of Gyrodactylus turnbulli (Monogenea) on guppies (Poecilia reticulata), Int. J. Parasitol., **37**, 375–381.

Gunay, A., Arslankaya, E. and Tosun, I. (2007) .Lead removal from aqueous solution by natural and pretreated clinoptilolite adsorption equilibrium and kinetics, J.Hazard. Mater., **146**, 362–371.

He, Z. L., Yang, X. E. and Stoffella, P. J. (2005) .Trace elements in agroecosystems and impacts on the environment. J. Trace Elem. Med. Biol., **19**, 125–140.

Jeon, Y. T., Lee, G. H., Park, J., Kim, B. and Chang, Y. (2005) .Magnetic Properties of Monodisperse NiHx Nanoparticles andComparison to those of Monodisperse Ni Nanoparticles. The Journal of Physical Chemistry B, **109**, 12257–12260.

Abu-Elella, R., Ossman, M. E., Abd-Elfatah , M. and Elgendy, A. (2013). Kinetic modeling and isotherm study for naphthalene adsorption on boehmite nanopowder. Desalination and Water Treatment journal, **51**, 3472-3481.

Asrari, E., Tavallali, H. and Hagshenas, M. (2010). Removal of Zn(II) and Pb (II) ions Using Rice Husk in Food Industrial Wastewater. J. Appl. Sci. Environ. Manage, **14 (4)**, 159 – 162.

Bansode, R. R., Losso, J. N., Marshall, W. E., Rao, R. M. and Portier, R. J. (2003). Adsorption of metal ions by pecan shell-based grsnular activated carbons, *J.* Biores. Technol., **89**, 115-119.

Bao, J. C., Tie, C. Y., Xu, Z., Zhou, Q. F., Shen, D. ,and Ma, Q. (2001). Template Synthesis of an Array of Nickel Nanotubules and Its Magnetic Behavior. Advanced Materials, **13 (21)**, 1631–1633.

Braos-Garcı´a, P., Maireles-Torres, P., Rodr'ıguez-Castello´ n, E., and Jime´nez-Lo´ pez, A. J. (2003). Gas-phase hydrogenation of acetonitrile on zirconium-doped mesoporous silica-supported nickel catalysts. Journal of Molecular Catalysis A. Chemical, **193**, 185–196.

Chien, S.H., and Clayton, W.R. (1980). Application of Elovich equation to the kinetics of phosphate release and sorption on soils. Soil Sci. Soc. Am. J., **44,** 265–268.

Dabrowski, A. (2001). Adsorption-from theory to practice, Adv. Colloid Interface Sci., **93**, 135–224.

Devaprasath, P. M., Solomon, J. S. and Thomas, B. V. (2007).Removal of Chromium (VI) from Aqueous Solutions using Natural Plant Mater. J. Appl. Sci. Environ. Sanitation, **2**, 77-83.

El-Sayed, G. O., Dessouki, H. A. and Ibrahiem, S. S. (2011). Removal Of Zn(II), Cd(II) And Mn(II) From Aqueous Solutions By Adsorption On Maize Stalks., The Malaysian Journal of Analytical Sciences, **15** , 21.

Gao, J. Z., Guan, F., Zhao, Y. C., Yang, W., Ma, Y. J., Lu, X. Q., Hou, J. G. and Kang, J. W. (2001). Preparation of Ultrafine Nickel Powder and its Catalytic Dehydrogenation Activity. Materials Chemistry and Physics, **71**, 215-219.

Jeon, Y. T., Moon, J. Y., Lee, G. H., Park, J. and Chang, Y. (2006). Comparison of the magnetic properties of metastable hexagonal close-packed Ni nanoparticles with those of the stable face-centered cubic Ni nanoparticles. The Journal of Physical Chemistry B, **110**, 1187–1191.

Kannan, N. and Veemraj T. (2009). Removal of Pb (II) ions by Adsorption onto Bamboo dust and Commercial Activated Carbons –A comparative study, E-J. Chem., **6**, 247-256.

Lagergren, S. (1898). Theorie der sogenannten adsorption geloster stoffe, Kungliga Svenska Vetenskapsakademiens. Handlingar, **24 (4)**, 1-39.

Liang, Z. H., Zhu, Y. J. and Hu, X. L. (2004). Nickel hydroxide nanosheets and their thermal decomposition to nickel oxide nanosheets. Journal of Physical Chemistry B, **108 (11)**, 3488–3491.

Lodeiro, P, Barriada, J.L., Herrero, R. and Sastre de Vicente M. E. (2006).The marine macro algae Cystoseira baccata as biosorbent forcadmium (II) and lead (II) removal, kinetic and equilibrium studies. Environmental Pollution, **142**, 264 273.

Mahmood, T., Saddique, M. T., Naeem, A., Mustafa, S., Dilara, B. and Raza, Z. A. (2011) .Cation exchange removal of Cd from aqueous solution by NiO, J. Hazard. Mater., **185** , 824–828.

Maximous, N. N., Nakhla G. F. and Wan, W. K. (2010). Removal of Heavy Metals from Wastewater by Adsorption and Membrane Processes a Comparative Study, World Academy of Science, Engineering and Technology 40.

Melitas, N., Chuffe-Moscoso, O. and Farrell, J. (2001). Kinetics of chromium removal from contaminated water by zerovalent iron media: corrosion inhibition and passive oxide effects, Environ. Sci. Technol., **35**, 3948–3953.

Moussa, H. A. (2004).Removal of heavy metals from wastewater by membrane processes a comparative study. Desalination, **164 (2)**, 105-110.

Ossman, M. E., Abdel Fatah, B. M. and Taha, A. N. (2013). Fe(III) removal by activated carbon produced from Egyptian rice straw by chemical activation. Desalination and Water Treatment journal, **52**, 3159-3168.

Pehlivan, E. and Altun, T. (2007). Ion-exchange of Pb^{2+}, Cu^{2+}, Zn^{2+}, Cd^{2+}, and Ni^{2+} ions from aqueous solution by Lewatit CNP 80. Journal of Hazardous Materials, **140**, 299–307.

Rafique, U., Imtiaz1, A. and Khan, A. (2012).Synthesis, Characterization and Application of Nanomaterials for the Removal of Emerging Pollutants from Industrial Waste Water&,Kinetics and Equilibrium Model. Journal of Water Sustainability, **2 (4)**, 233-244.

Reddad, Z., Gerente, C., Andres, Y. and LeCloirece, P. (2002). Adsorption of several metal ions onto a low-cost biosorbent: kinetic and equilibrium studies. *J.* Environ. Sci. & Technol., **36 (9)**, 2067- 2073.

Seto, T., Akinaga, H., Takano, F., Koga, K., Orii, T. and Hirasawa, M. (2005).Magnetic properties of monodispersed Ni/NiO core-shell nanoparticles. Journal of Physical Chemistry B, **109 (28)**, 13403–13405.

Shanmugavalli R., Syed Shabudeen P. S., Venckatesh R., Kadirvelu K., Madhavakrishnan S. and Pattabhi S. (2009).Uptake of Pb (II) ion From Aqueous Solution Using Silk Cotton Hull Carbon: An Agricultural Waste Biomass, E-J. Chem., **3**, 218-229.

Shipley, H. T., Engates , K. E. and Grover, V. A. (2013). Removal of Pb(II), Cd(II), Cu(II), and Zn(II) by hematite nanoparticles: effect of sorbent concentration, pH, temperature, and exhaustion, Environ Sci Pollut Res Int., **20 (3)**, 1727-36.

Sun, S., Murray, C. B., Weller, D., Folks, L. and Moser, A. (2000). Monodisperse Fe-Pt nanoparticles and ferromagnetic FePt nanocrystal superlattices. Science, 287(5460).

Tian, F., Zhu, J., Wei, D. and Shen, Y.T. (2005). Magnetic field assisting DC electrodeposition:general methods for highperformanceNi nanowire array fabrication. Journal of Physical Chemistry B, **109 (31)**, 14852–14854.

Wang, Y.,(2000) .Microbial reduction of chromate, in: D.R. Lovley (Ed.), Environmental Microbe – Metal Interactions, American Society for Microbiology Press, Washington, 225–235.

Weber, W. J. and Morris, J. C. (1963). Kinetics of adsorption on carbon from solution. J. Sanity Eng. Div. Am. Soc. Civil Eng., **89**, 31–59.

Wong, K. K., Lee, C. K., Low, K. S. and Haron, M. (2003). Removal of Cu and Pb by tartaric acid modified rice husk from aqueous solution. J. Chemospere, **50**, 23-28.

Yemane, M.and Chandravanshi, B.S. (2008). Levels of essential and non-essential metals in leaves of the tea plant (Camellia sinensis L.) and soil of Wush farms, Ethiopia, Food Chem., **107**, 1236–1243.

Zeng, G., Pang, Y., Zeng, Z., Tang, L., Zhang, Y., Liu, Y., Zhang, J., Lei, X., Li, Z., Xiong, Y. and Xie, G. (2011) . Removal and recovery of Zn2+ and Pb2+ by imine-functionalized magnetic nanoparticles with tunable selectivity. Langmuir, **28**, 468–473.